

## Elastic scattering of 19.5 and 30 MeV negative pions from $^{12}\text{C}$

D. H. Wright and M. Blecher

*Virginia Polytechnic Institute and State University, Blacksburg, Virginia 24061*

R. L. Boudrie, R. L. Burman, and M. J. Leitch

*Los Alamos National Laboratory, Los Alamos, New Mexico 87545*

B. G. Ritchie and D. Rothenberger

*Arizona State University, Tempe, Arizona 85287*

Z. Weinfeld

*Tel Aviv University, Ramat Aviv, Israel*

M. Alsolami, G. Blanpied, J. A. Escalante, C. S. Mishra,\* G. Pignault,† B. M. Preedom, and  
C. S. Whisnant

*University of South Carolina, Columbia, South Carolina 29208*

(Received 24 March 1987)

Elastic cross sections for the scattering of negative pions from  $^{12}\text{C}$  were measured at 19.5 and 30 MeV incident pion energy. At both energies the new cross sections show fair agreement with optical model predictions. At 30 MeV the new cross sections disagree at forward angles with previously measured values, while at 19.5 MeV the data represent the first report of  $^{12}\text{C}$   $\pi^-$  scattering at this energy.

Negative pion scattering from  $^{12}\text{C}$  constitutes a test of low energy pion-nucleus optical potentials whose parameters have been determined largely from  $\pi^+$  scattering. Reliable elastic pion scattering data from  $^{12}\text{C}$  are also important because they are often used to normalize inelastic scattering in  $^{12}\text{C}$  as well as to normalize elastic scattering in other nuclei. In this article 19.5 and 30 MeV  $\pi^-$  elastic scattering data for  $^{12}\text{C}$  are presented and compared to the 19.5 and 30 MeV predictions of the MSU (Ref. 1) and PIESDEX (Ref. 2) potentials. The 30 MeV data are also compared to the earlier data of Johnson.<sup>3</sup>

The data were collected with the Clamshell spectrometer<sup>4</sup> on the Low Energy Pion channel at the Clinton P. Anderson Meson Physics Facility (LAMPF). The spectrometer has a full angular acceptance of  $12^\circ$  and an estimated scattering angle uncertainty of  $\pm 0.2^\circ$ . Its acceptance varies linearly with position on the focal plane over a range of  $\pm 15\%$  of the spectrometer's central momentum and cross sections are corrected for this effect.

The relative incoming pion flux was determined by a toroidal current monitor of the proton beam located upstream of the pion production target and by  $\pi\mu$  decay telescopes<sup>5</sup> located near the beam and just upstream of the spectrometer scattering target.

In the 30 MeV experiment negative pions struck a  $236\text{ mg/cm}^2$   $\text{CH}_2$  target and were detected at lab angles between  $23^\circ$  and  $108^\circ$ . The pion energy at the center of the target was 30 MeV, and the momentum acceptance of the LEP channel was 1% FWHM (full width at half maximum). Cross sections were collected in  $6^\circ$  bins of

the lab scattering angle and then corrected for the finite solid angle.  $^{12}\text{C}$  cross sections were normalized to the FA86  $\pi\text{p}$  phase shift cross sections of Arndt and Roper.<sup>6</sup> Because the  $\pi^-$ p measurements were obtained from the  $\text{CH}_2$  target simultaneously with the  $^{12}\text{C}$  cross sections, systematic errors in the normalization were reduced, resulting in a normalization uncertainty of  $\pm 6\%$ . The individual data points typically have error bars of  $\pm 3\%$ , which represent only the counting statistics. All other errors combined, with the exception of the normalization error, were estimated to be less than 1%. The data are presented in Table I.

In the 19.5 MeV experiment negative pions struck a  $225\text{ mg/cm}^2$   $^{12}\text{C}$  target and were detected at lab angles between  $30^\circ$  and  $110^\circ$ . In this case the momentum acceptance of the LEP channel was 2% FWHM and 19.5 MeV was the pion energy at the center of the target. Cross sections were collected in  $8^\circ$  bins of the lab scattering angle and then corrected for the finite solid angle. Cross sections for  $\pi^-$ p at 19.5 MeV were obtained by scattering from a  $142\text{ mg/cm}^2$   $\text{CH}_2$  target. Use of the FA86  $\pi^-$ p phase shift cross sections of Arndt and Roper<sup>6</sup> yielded a  $^{12}\text{C}$  normalization known to within  $\pm 7\%$ . The individual data points have typical error bars of  $\pm 4\%$ , again reflecting only the counting statistics. As in the 30 MeV case, other errors were estimated to be small. The low energy of the incident pions and the 2 m flight path in the spectrometer ensured a clean separation by time of flight of the pions and muons, thus avoiding muon contamination of the elastic pion peak even at forward angles. Pion identification was determined by accumulating a spectrum of particle transit times from a 1.59

TABLE I. 30 MeV  $^{12}\text{C}(\pi^-, \pi^-)$  cross sections.<sup>a</sup>

$\theta_{\text{c.m.}}$	$d\sigma/d\Omega$ (mb/sr)	Error (mb/sr)
23.6	59.9	1.8
29.0	34.6	1.2
40.3	12.3	0.3
44.7	7.73	0.26
48.8	6.13	0.34
55.0	2.02	0.09
68.4	1.13	0.05
76.7	1.35	0.06
82.0	1.83	0.06
92.5	3.21	0.08
102.8	4.41	0.15
108.3	5.08	0.16

<sup>a</sup> Normalization uncertainty of  $\pm 6\%$  not included.

mm thick scintillator at the entrance of the spectrometer to the first of two large area, 6.32 mm thick trigger scintillators near the spectrometer focal plane. A typical spectrum with the pion time of flight cut is shown in Fig. 1. The 19.5 MeV data are presented in Table II.

The new data are compared in Fig. 2 to the predictions at 30 MeV of the MSU and PIESDEX potentials. The solid curve was generated using MSU parameter set E at 25 and 50 MeV interpolated to 30 MeV, and nuclear density parameters for  $^{12}\text{C}$  which are derived from electron scattering<sup>7</sup> and corrected for finite proton and pion sizes.

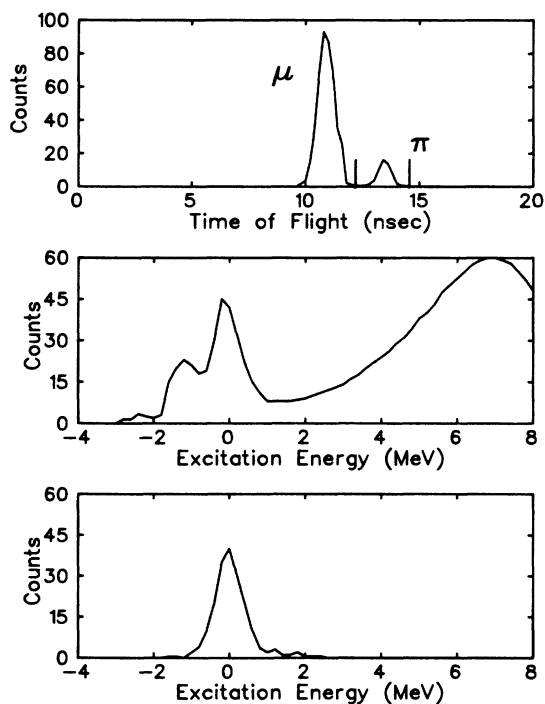


FIG. 1. Top: Pion time-of-flight cut for  $^{12}\text{C}(\pi^-, \pi^-)$  at 19.5 MeV and  $40^\circ$  scattering angle. Middle: excitation spectrum without TOF cut. Bottom: excitation spectrum with TOF cut.

TABLE II. 19.5 MeV  $^{12}\text{C}(\pi^-, \pi^-)$  cross sections.<sup>a</sup>

$\theta_{\text{c.m.}}$	$d\sigma/d\Omega$ (mb/sr)	Error (mb/sr)
28.6	49.6	3.0
38.7	13.0	0.4
48.8	4.54	0.14
58.8	1.50	0.06
68.9	0.82	0.08
78.9	1.40	0.09
88.9	2.42	0.12
98.9	3.94	0.15
108.8	5.48	0.21

<sup>a</sup> Normalization uncertainty of  $\pm 7\%$  not included.

Very good agreement with the data is obtained at forward angles. At all angles past the minimum the present data are consistently overestimated by the prediction. The dashed curve was generated using the PIESDEX code of Siciliano *et al.* with Skyrme III nuclear densities and the potential parameters of Alons *et al.* (Table III).<sup>8</sup> This potential describes the data somewhat better in the region of the minimum but still overshoots it at backward angles. Note that for elastic scattering on  $T=0$  nuclei the PIESDEX and MSU potentials are, in principle, identical and their parameters simply related as shown in Tables III and IV. The main difference is that the PIESDEX isoscalar  $\rho^2$  parameters  $\lambda_{s0}^{(2)}, \lambda_{p0}^{(2)}$  were obtained by fits to elastic scattering data from  $T=0$  nuclei in the range 20–80 MeV.<sup>8</sup> The imaginary parts of the corresponding MSU parameters  $B_0, C_0$  were determined by setting  $\text{Im}C_0$  to 60% of its pionic atom value and fixing the ratio  $\text{Im}B_0/\text{Im}C_0$  at its pionic atom value; the real parts were determined by theoretical estimates.

Comparing the present data at 30 MeV to that of Johnson *et al.*<sup>3</sup> in Fig. 3 shows that the Johnson data at forward angles are about 70–50% of the optical model

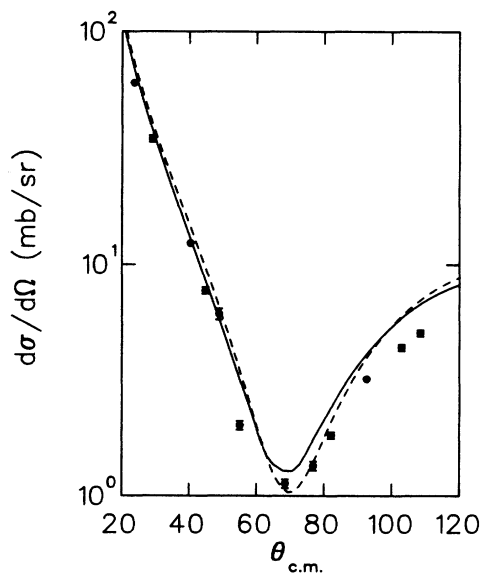
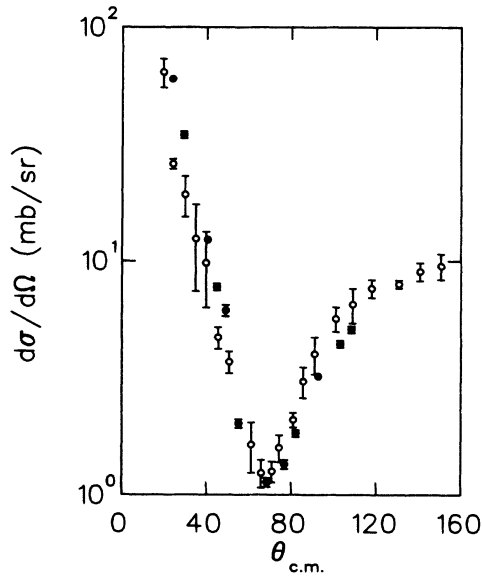
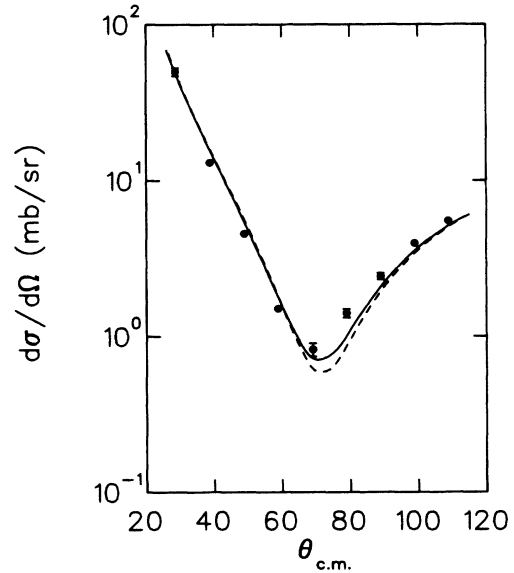


FIG. 2.  $^{12}\text{C}(\pi^-, \pi^-)$  data at 30 MeV compared with the predictions of the MSU potential (solid curve) and the PIESDEX potential (dashed curve).

TABLE III. PIESDEX potential parameters.

	30 MeV parameters	19.5 MeV parameters	Relation to MSU parameter
$\lambda_{s0}^{(1)}$	(-3.565, 0.155)	(-4.742, 0.113)	$b_0 = \lambda_{s0}^{(1)}(k^2/4\pi p_1)$
$\lambda_{s1}^{(1)}$	(-15.384, -0.008)	(-23.961, -0.020)	$b_1 = \lambda_{s1}^{(1)}(k^2/8\pi p_1)$
$\lambda_{p0}^{(1)}$	(6.992, 0.071)	(6.629, 0.021)	$c_0 = \lambda_{p0}^{(1)}(p_1/4\pi)$
$\lambda_{p1}^{(1)}$	(10.253, 0.065)	(10.464, 0.019)	$c_1 = \lambda_{p1}^{(1)}(p_1/8\pi)$
$\lambda_{s0}^{(2)}$	(0.068, 0.657)	(-0.437, 1.993)	$B_0 = \lambda_{s0}^{(2)}(k^2/4\pi p_2 \rho_0)$
$\lambda_{s1}^{(2)}$	(0.0, 0.0)	(0.0, 0.0)	$B_1 = \lambda_{s1}^{(2)}(k^2/8\pi p_2 \rho_0)$
$\lambda_{p0}^{(2)}$	(1.493, 0.915)	(1.427, 0.749)	$C_0 = \lambda_{p0}^{(2)}(p_2/4\pi\rho_0)$
$\lambda_{p1}^{(2)}$	(0.0, 0.0)	(0.0, 0.0)	$C_1 = \lambda_{p1}^{(2)}(p_2/8\pi\rho_0)$

$p_1 = (1 + \epsilon)/(1 + \epsilon/A), \quad p_2 = (1 + \epsilon/2)/(1 + \epsilon/A)$   
 $\epsilon = (k^2 + m^2)^{1/2}/M_N, \quad \rho_0 = 0.16 \text{ fm}^{-3}$

FIG. 3. The present  $^{12}\text{C}(\pi^-, \pi^-)$  data at 30 MeV (closed circles) compared to the previous measurements of Johnson (open circles).FIG. 4.  $^{12}\text{C}(\pi^-, \pi^-)$  data at 19.5 MeV compared with the predictions of the MSU potential (solid curve) and the PIESDEX potential (dashed curve).TABLE IV. Comparison of MSU and PIESDEX parameters.<sup>a</sup>

	30 MeV		19.5 MeV	
	MSU	PIESDEX	MSU	PIESDEX
$b_0$	(-0.055, 0.002)	(-0.056, 0.002)	(-0.051, 0.001)	(-0.048, 0.001)
$b_1$	(-0.130, -0.001)	(-0.120, 0.000)	(-0.130, -0.001)	(-0.120, 0.000)
$c_0$	(0.684, 0.010)	(0.639, 0.006)	(0.676, 0.005)	(0.608, 0.002)
$c_1$	(0.443, 0.005)	(0.469, 0.003)	(0.437, 0.003)	(0.480, 0.001)
$B_0$	(-0.009, 0.153)	(0.041, 0.071)	(-0.003, 0.168)	(-0.030, 0.135)
$B_1$	(0.000, 0.000)	(0.000, 0.000)	(0.000, 0.000)	(0.000, 0.000)
$C_0$	(0.327, 0.688)	(0.788, 0.483)	(0.312, 0.775)	(0.759, 0.399)
$C_1$	(0.000, 0.000)	(0.000, 0.000)	(0.000, 0.000)	(0.000, 0.000)

<sup>a</sup> PIESDEX parameters have been converted to the MSU format.

predictions, while the present data agree quite well with those predictions. For angles of  $60^\circ$  and greater the Johnson data set agrees with the optical model predictions and the present data agree within uncertainties to the Johnson set but fall below the optical model curves.

The 19.5 MeV  $\pi^{-12}\text{C}$  data are shown in Fig. 4, where they are compared to the predictions of the MSU and PIESDEX optical potentials. As for the 30 MeV data, the MSU potential employs parameter set E interpolated for 19.5 MeV and the PIESDEX potential uses the parameters of Alons *et al.* The curves generated by the potential are nearly identical, with PIESDEX producing the deeper minimum and agreeing only slightly less well with the data than does the MSU potential. For scattering angles forward of  $60^\circ$  (the  $s$ - $p$  interference minimum) the curves overestimate the data by 10–20% with the exception of the most forward point which is well reproduced. Beyond  $60^\circ$  the data agree better with the MSU prediction, where it and the PIESDEX prediction describe the data better as the scattering angle increases.

The data also suggest a slight shift of the minimum to a smaller-than-predicted scattering angle.

The following conclusions can be drawn from the present work: (1) 19.5 and 30 MeV  $\pi^{-12}\text{C}$  cross sections are fairly well described by both MSU and PIESDEX potentials. The 30 MeV data are well described at forward angles and overestimated in the  $s$ - $p$  interference minimum and at backward angles, while the 19.5 MeV data are overestimated at forward angles and underestimated at backward angles.

(2) The MSU and PIESDEX potentials, which for elastic scattering are identical in form, use different sets of parameters but do not differ significantly in their predictions of the 19.5 and 30 MeV  $\pi^{-12}\text{C}$  angular distributions.

This work was supported by grants from the U.S. National Science Foundation (ASU, USC, VPI and SU) and by the U.S. Department of Energy (LANL).

---

\*Present address: Physics Division p-2, Mail Stop D456, Los Alamos National Laboratory, Los Alamos, NM 87545.

†Present address: 22 Rue Lucces, Chaurpionuieu, 75013 Paris, France.

<sup>1</sup>J. A. Carr, H. McManus, and K. Stricker-Bauer, *Phys. Rev. C* **25**, 952 (1982).

<sup>2</sup>E. R. Siciliano M. D. Cooper, Mikkel B. Johnson, and M. J. Leitch, *Phys. Rev. C* **34**, 267 (1986); M. B. Johnson and E. R. Siciliano, *ibid.* **27**, 1647 (1983).

<sup>3</sup>R. R. Johnson *et al.*, *Phys. Rev. Lett.* **43**, 844 (1979).

<sup>4</sup>B. Fick *et al.*, *Phys. Rev. C* **34**, 643 (1986).

<sup>5</sup>E. A. Wadlinger, *Nucl. Instrum. Methods* **134**, 243 (1976).

<sup>6</sup>R. A. Arndt and L. D. Roper, program SAID, Center for Analysis of Particle Scattering, Virginia Polytechnic Institute and State University, 1986.

<sup>7</sup>C. W. deJager, H. DeVries, and C. DeVries, *At. Data Nucl. Data Tables* **14**, 479 (1974).

<sup>8</sup>P. W. F. Alons, M. J. Leitch, and E. R. Siciliano (unpublished).